

¹ **Characterizing precipitation behaviors from recent historical climate to 21st
² Century over Western United States**

³ Xingying Huang, * Paul A. Ullrich

⁴ *Department of Land, Air and Water Resources, University of California, Davis*

⁵ *Corresponding author address: Xingying Huang, Department of Land, Air and Water Resources,
⁶ University of California Davis, Davis, CA 95616.
⁷ E-mail: xyhuang@ucdavis.edu

ABSTRACT

8

9 **1. Introduction**

10 Precipitation changes have always been an important issue that bring a lot attention in climate
11 modeling studies, due to the significant impacts of precipitation related phenomenon especially for
12 drought occurrence and heavy precipitation events (Seneviratne et al. 2012). There are a number
13 of studies aiming to find out how the precipitation will behave in future based on varied climate
14 forcing scenarios under anthropogenic-induced changes (Hegerl et al. 2004; Kharin et al. 2007;
15 Scoccimarro et al. 2013), stating that the world is getting wetter relating with a warmer climate.
16 However, the impacts of climate change vary regionally in their severity, with more attention need
17 to be paid on regional climate extremes study to make effective responses.

18 Although prediction of future climate has large uncertainty, climate model simulations are
19 nonetheless the most useful information we can resort to study potential climate variability and
20 extremes changes in future (Easterling et al. 2000). Global climate models (GCMs) are primarily
21 used to investigate possible future changes in mean climate mean, variability and extremes, forced
22 with projected greenhouse gas concentration and aerosol emissions. There are a large amount
23 studies and results concerning the global changes of climate extremes (Seneviratne et al. 2012),
24 but much less efforts focusing on the regional scale which is needed in order to implement cli-
25 mate adaptation and mitigation strategies. Due to the coarse resolutions ($\sim 1^\circ$) of GCMs, regional
26 climate models (RCMs) are mostly used to get the frequency, intensity, and duration of extreme
27 events, by better capturing fine-scale dynamical features with high horizontal resolution (Bell et al.
28 2004; Frei et al. 2006; Rauscher et al. 2010; Wehner 2013). Higher resolution can allow better
29 simulation of precipitation extremes, related with regional representation in land use, landwater
30 contrast, snow cover, cloudiness and circulation patterns associated with fine topography (Leung
31 et al. 2003a; Diffenbaugh et al. 2005; Salathé Jr et al. 2008; Wehner et al. 2010).

32 Except RCMs, variable-resolution enabled GCMs (VRGCMs) are also one of the dynamical
33 downscaling methods that has been receiving a growing interest in modeling regional climate re-
34 cently. Unlike RCMs, which are forced by the output from GCMs for future projections, VRGCMs
35 use a relatively coarse global model with enhanced resolution over a specific region (Staniforth
36 and Mitchell 1978; Fox-Rabinovitz et al. 1997), demonstrating utility for regional climate studies
37 and applications at a reduced computational cost compared to uniform-resolution GCMs (Fox-
38 Rabinovitz et al. 2006; Rauscher et al. 2013). Contrasted with RCMs, VRGCMs use a single,
39 unified modeling framework rather than two separate models (GCM and RCM) with potentially
40 disparate dynamics and physics parameterizations, avoiding the inconsistencies and lack of two-
41 way interactions between the global and regional scales at the nest boundary of RCMs (McDonald
42 2003; Laprise et al. 2008; Mesinger and Veljovic 2013).

43 For our purpose, we use the recently developed variable-resolution option in Community Earth
44 System Model (VR-CESM) to get the potential changes of precipitation extremes till end of 21st
45 century over western U.S. For decades, CESM (and its predecessor, the Community Climate Sys-
46 tem Model) has been used for modeling present and future global climate (Neale et al. 2010a;
47 Hurrell et al. 2013). The overall performance of VR-CESM in modeling California's climate has
48 been addressed in detail in Huang et al. (2016), which demonstrates VR-CESM has competitive bi-
49 ases when compared with a regional climate model forced by reanalysis data, as evaluated against
50 high-quality observations and reanalysis datasets. VR-CESM has also been employed by other
51 studies showing the comparable ability in capturing fine-scale atmospheric processes as uniform
52 CESM or a RCM, and do not exhibit apparent artifacts in the variable-resolution transition region
53 (Rhoades et al. 2015; Zarzycki et al. 2014, 2015).

54 Overall, in this paper, we focus on investigate the changes of precipitation behaviors during
55 21st Century over western U.S. based on long-term ensemble runs conducted by VR-CESM at

56 the resolution of 0.25° . Simulations are performed following the RCP (reference concentration
57 pathways) 8.5 scenario, representing the highest rate of increase in greenhouse gas concentrations
58 within the new set of RCPs. We anticipate to obtain the changes of overall precipitation and the
59 upper bound of the precipitation events distribution under warmer climate with high-resolution
60 simulation output from the recent-climate to the end of 21st Century. This study aims to further
61 improve our understanding of both past and future regional precipitation behaviors at fine-scale.

62 (add more text here)

63 This paper is structured as following. Section 2 describes the model setup, methodology and
64 reference datasets used. Results are presented and analyzed in Section 3 including the model
65 evaluation, mean climatology trend and precipitation extremes changes. Section 4 summarizes the
66 main points of the study along with detailed discussion.

67 (add the hypothesis we want to argue here) (a) the choice of index b) the use of VR-CESM c)
68 study of the ENSO and climate forcing together)

69 **2. Models and Methodology**

70 *a. Model setup*

71 As above-mentioned, CESM, as a state-of-the-art Earth modeling framework, consists of cou-
72 pled atmospheric, oceanic, land and sea ice models (Neale et al. 2010b; Hurrell et al. 2013). In
73 this study, Community Atmosphere Model version 5 (CAM5) (Neale et al. 2010b) and the Com-
74 munity Land Model version 4.0 (Oleson et al. 2010) are used. CAM 5 is driven by the Spectral
75 Element (SE) dynamical core with conservation and parallel scaling properties (Dennis et al. 2011;
76 Taylor 2011) and supporting variable-resolution option (Zarzycki et al. 2014). Global sea-surface
77 temperatures and sea ice are prescribed in accordance with the Atmospheric Model Intercompar-

78 ison Project (AMIP) protocol (Gates 1992), which are widely used and support climate model
79 diagnosis, validation and intercomparison. The finest horizontal resolution of our grid is \sim 28 km
80 covering the western U.S., with a quasi-uniform 1° mesh over the remainder of the globe (See
81 Figure 1). A detailed description of the techniques of VR-CESM employed in this paper including
82 the grids generation, topography preparation and component set can be found in Rhoades et al.
83 (2015); Huang et al. (2016).

84 Simulations have been conducted for both historical climate and transient future projections .
85 The historical climate simulation cover the period 1979 through 2005. The transient future projec-
86 tions cover two periods including near future 2024-2050 and late-century 20692095. For purposes
87 of analysis, the first year of each time period was discarded as a spin-up period to allow adequate
88 time for the initialized land and atmosphere to equilibrate. The 26-year duration was chosen to
89 provide an adequate sampling of annual variability for each time phase. For future projections,
90 GHG concentrations are set based on RCP 8.5 senario which describes GHG emissions continue
91 to rise throughout the 21st century (Riahi et al. 2011). Simulations are forced by observed sea-
92 surface temperatures (SSTs) and sea ice for historical period at 1° as described by Hurrell et al.
93 (2008), and simulated SSTs and sea ice for future projections are provided by Hannay ([add cita-](#)
94 [tion](#)), without the added complexity of ocean-atmosphere feedbacks in the climate system. Land
95 surface datasets, including plant functional types, at 0.5° were adopted for each year.

96 Due to the uncertainty in future climate projections, ensemble simulations are needed, especially
97 for climatology statistics associated with temperature and precipitations. However, due to the
98 diverse internal variability for different climate models and for different climate variables, there is
99 no standard criteria for the minimum number of simulations needed for climate extremes studies
100 (Deser et al. 2012). According to Ryan L. Sriver et al. (2014) ([add citation](#)), CESM ensemble
101 show obviously smaller uncertainty than Coupled Model Intercomparison Project Phase (CMIP)

102 5 for both temperature and precipitation in North America. Based on the results of Deser et al.
103 (2012), at least three ensemble runs are required to detect a significant epoch difference for the JJA
104 surface temperature, and for precipitation, more than 40 ensemble runs are needed. Considering
105 that we did not explicitly use coupled ocean model and we focused on regional area at much finer
106 resolution, in this study, we did four simulations for each future time period. We also have two
107 runs for the historical period. Due to the relatively small uncertainty within the runs over the same
108 time period (shown by the supplement), we assume that the numbers of ensemble runs applied in
109 this study are enough to satisfy our goal.

110 plot in supplement: the relative difference between specific run and ensemble mean of different
111 period

112 3. Methodology

113 In order to thoroughly capture the frequency, intensity, and duration of precipitation events dis-
114 tribution at each time period, we used all the daily precipitation data of our simulations since strong
115 precipitation events can occur in different seasons for diverse climate divisions. As a common ap-
116 proach, extreme indices are employed to depict the behaviors of precipitation (Tebaldi et al. 2006;
117 Zhang et al. 2010; Duli  re et al. 2011; Zhang et al. 2011; Sillmann et al. 2013). In our study, we
118 have tried many relevant indices including those defined by the Expert Team on Climate Change
119 Detection and Indices (ETCCDI) and others used in previous studies depicting the percentiles,
120 maximum value, or the events changes of Pr. It turned out that those are suitable for our purpose
121 here, since we assume that the indices used should be suitable, easily interpreted and being rele-
122 vant for policy makers. Therefore, we end up with the indices summarized in Table 1 defining the
123 different ranges of precipitation distributions.

124 Due to the important role ENSO plays in regulating the precipitation over southwest U.S. (add
125 citation here zhang2010influence, deser2012communication), the phase of ENSO (El Nino and La
126 Nina) over each year is identified by the Nino 3.4 index. Some papers discuss that Nino 3.4 can
127 not capture ENSO well, like Kao and Yu (2009), we tried to widen the location (from 170W to
128 105W rather than from 170W to 120W) a little bit, the SST anomaly of each year is quite similar
129 to what we got from Nino 3.4, especially for future periods. Therefore, we presume it won't really
130 affect our results whether the location extends or not.

131 (The values of Nino index: see supplement. *indices_oni.pdf* (update this figure))

132 (add description of the supplement)

133 a. Reference datasets

134 UW, CPC, NARR

135 (add the descriptions of these datasets here)

136 4. results

137 a. evaluation

138 In order to see whether the model can capture the mean features of precipitation distribution, the
139 results from VR-CESM and references are shown in Figure 2 including the mean precipitation and
140 related indices. The fractions of rain amount for total Pr attributed by corresponding indices are
141 also added in this figure to figure out the contribution of water of different ranges of Pr intensity.

142 It can be seen that compared to observations, VR-CESM can well reproduce the spatial patterns
143 of precipitation with quite similar magnitude, considering the uncertainty within these references.

144 We also notice that CESM tends to overestimate the precipitation over the eastern side of the
145 Cascades and the northern western side of the Sierra Nevada and overestimate the precipitation

146 over the part of the Great Plains and the New Mexico, for precipitation rate under 20 mm/day.
147 Biases in simulating extreme precipitation over the topographically complex regions have been
148 found Singh et al. (2013), being attributed to excessively strong winds. Most of the rain over dry
149 area is obtained from non-extreme Pr (with $Pr < 10\text{mm}$), while most of the precipitation over wet
150 area is from extreme Pr (when $Pr > 10\text{mm}$).

151 *b. mean climatology*

152 Before getting into the analysis of the changes of precipitation features, it is important to un-
153 derstand the overall mean changes of precipitation and other relevant background variables. Since
154 majority of the precipitation is from rainy seasons overing October to March (see Pr_monthly.pdf
155 in the supplement), Pr from each time period is depicted in each half of the year including the wet
156 season from October to March and the dry season from April to September as we defined (see
157 Figure 3).

158 Though temperature increases along with enhanced GHGs concentration, mean precipitation did
159 not show notable changes. Mean precipitation tends to increase lightly over the northern western
160 U.S during wet season, and over the central and southern part of WUS during dry season. There
161 is a minor decrease of total precipitation over the Cascades and its western side during dry season,
162 and also a light decrease of overall precipitation over part of the Sierra Nevada. No significant
163 trend is observed for mean precipitation within each time period.

164 As mean temperature goes up, there is consistent increase of 2m relative humidity over coastal
165 region and west side of the Sierra Nevada in future, and slight decrease over most of the region
166 during wet seasons. For dry seasons, the 2m relative humidity has slight increase over central-
167 southern part of WUS during mid-century, and overall decrease over the remaining study area,
168 especially during end-century. As argued by Joshi et al. (2008), water vapor content over land

¹⁶⁹ does not increase fast enough relative to the rapid warming so that relative humidity will decrease
¹⁷⁰ on average, as also seen in other model simulations (Rowell and Jones 2006) and observed on all
¹⁷¹ continents (Simmons et al. 2010).

¹⁷² (update *pr_mean_clm.pdf* using all the runs)

¹⁷³ *c. Precipitation*

¹⁷⁴ Given continuously increases of temperature in future, here the changes of precipitation features
¹⁷⁵ are displayed in Figure 4 including the differences between historical time period and future. It
¹⁷⁶ can be seen that precipitation distribution shows consistent trend of changes when going into
¹⁷⁷ mid of 21st century and till end of 21st century. The overall rainy days and frequency of non-
¹⁷⁸ extreme precipitation (i.e. with daily Pr no large than 10 mm) have decreased lightly over the
¹⁷⁹ northern western U.S and California, and increased over the central and southern part of WUS,
¹⁸⁰ and this feature is mainly caused by the changes over dry seasons. As for the extreme precipitation
¹⁸¹ frequency (i.e. with daily Pr between 10 mm and 40 mm), there is a decreasing trend over the
¹⁸² Cascades and part of the Sierra Nevada, and a more obvious increasing trend over the northern
¹⁸³ western coast and eastern side of the Cascades. For the very extreme precipitation events, there is
¹⁸⁴ a notable increasing trend over the northern western coast and the Cascades, and a slight decrease
¹⁸⁵ over part of the Sierra Nevada. The decrease of rainy days during hot and dry season over central
¹⁸⁶ southern California, though with a minor magnitude, will probably intensify the drought condition
¹⁸⁷ due to the deficit of soil moisture due to higher evapotranspiration caused by the warmer climate
¹⁸⁸ in the future, as also found by Cayan et al. (2010); Bell et al. (2004).

¹⁸⁹ (update the figures in discussion.pdf, add ivt and iwv when daily $40 \text{ mm} \geq pr > 20 \text{ mm}$ and
¹⁹⁰ when $pr > 40 \text{ mm}$; might add the Z500 contour to the plot or Sea level pressure) add descriptions
¹⁹¹ here.

192 In order to investigate the impacts of large scale variability by ENSO, the difference of precipi-
193 tation behaviors between the warm phase (i.e. El Nino) and cool phase (i.e. La Nina) of ENSO is
194 illustrated in Figure 5 during the wet season. It can be found that during El Nino phase, higher pre-
195 cipitation intensity is expected over southwest U.S. (Hamlet and Lettenmaier 2007), and smaller
196 precipitation intensity over the northwest U.S., forming a dipole effect of ENSO. This feature is of-
197 ten characterized as a northwest/southwest precipitation dipole, causing by the effects of ENSO on
198 cool season precipitation through the storm track behavior (Gershunov and Barnett 1998; Leung
199 et al. 2003b), modulating the enhanced precipitation variability in the southwestern U.S. (Cayan
200 and Webb 1993; Cayan et al. 1999; Kahya and Dracup 1994).

201 This is further proved in the Figure 6 including the vertically integrated vapor transport (IVT)
202 and integrated water vapor (IWV), due to the major contribution of precipitation by atmospheric
203 rivers over West Neiman et al. (2008); Ralph et al. (2004); Leung and Qian (2009); Dettinger
204 (2011).

205 The precipitation frequency also show increase over southwest U.S., and decrease over the north-
206 west region. In future, the impact of ENSO tends to intensify, which seems to be related with the
207 changes of the strength of El Nino and La Nina. This can be explained by the SST anomaly values
208 (detrended) of warm and cold phases (see the supplement). The impact of ENSO for observational
209 precipitation has a weaker signal of the dipole effect compared to the CESM (see the supplement),
210 which might suggest that the model has a overestimation of the ENSO effect on precipitation,
211 especially over the northwest U.S. (add descriptions here based on the discussion.pdf)

212 **5. Discussion and Summary**

213 In this study, North Pacific Oscillation (NPO) is not analyzed due to its decades duration making
214 it hard to be well captured over 26 years time period. Further, as argued by Pierce (2002) the NPO

215 turned out to respond to the same internal atmospheric variability as ENSO, therefore, no signif-
216 icant improvement can be obtained to account for the ENSO's effects by incorporating accurate
217 predictions of NPO SSTs.

218 Kim (2005) found that under global warming, heavy precipitation events show largest increases
219 in the mountainous regions of the northern California Coastal Range and the Sierra Nevada. How-
220 ever, our results show a decrease of extreme precipitation over the Sierra Nevada. As suggested by
221 Hamlet and Lettenmaier (2007), global warming has played a relatively minor role in determining
222 cool season precipitation trends over historic period with an obvious change in the interannual
223 variability across the West. In our study, the signal of global warming in regulating the behav-
224 iors of precipitation is also not as obvious as the impact of large scale variability (i.e. ENSO).
225 Although the human-induced increases in greenhouse gases have been attributed to the observed
226 intensification of heavy precipitation events over tropical ocean (Allan and Soden 2008) or over
227 majority of the Northern Hemisphere land areas Min et al. (2011), the contribution could diverse
228 largely regionally due to atmospheric circulation patterns of variability (Trenberth 2011), which
229 can not be accurately described by coarse resolution used in the previous studies.

230 According to previous studies (e.g. (Allen and Ingram 2002; Allan and Soden 2008; O'Gorman
231 and Schneider 2009; Min et al. 2011)), changes in more extreme precipitation follow the Clausius-
232 Clapeyron relationship, i.e. the atmospheric water vapor content increases at an approximate rate
233 of 7.5% per kelvin of atmospheric temperature, more closely than total precipitation precipitation
234 amount (Trenberth et al. 2003). Based on CMIP3 simulation, Kharin et al. (2007) argued that
235 there will be an increase of annual one day maximum precipitation (Max1d) for about 6% with
236 each kelvin of global warming, with ranging of 4%-10% K with the models. We see the changes
237 of the strength of ENSO in future in CESM, which has been a debate that El Nino will change
238 under global warming by altering the background climate by plenty of studies (Fedorov and Phi-

²³⁹ lander 2000; Guilyardi et al. 2009). Yoon et al. (2015) found that the projected increase in water
²⁴⁰ cycle extremes including intense drought and excessive flooding in California is associated with
²⁴¹ a strengthened relation to ENSO not only through its warm and cold phases but also its precursor
²⁴² patterns.

²⁴³ *Acknowledgments.*

²⁴⁴ **References**

²⁴⁵ Allan, R. P., and B. J. Soden, 2008: Atmospheric warming and the amplification of precipitation
²⁴⁶ extremes. *Science*, **321** (5895), 1481–1484.

²⁴⁷ Allen, M. R., and W. J. Ingram, 2002: Constraints on future changes in climate and the hydrologic
²⁴⁸ cycle. *Nature*, **419** (6903), 224–232.

²⁴⁹ Bell, J. L., L. C. Sloan, and M. A. Snyder, 2004: Regional changes in extreme climatic events: a
²⁵⁰ future climate scenario. *Journal of Climate*, **17** (1), 81–87.

²⁵¹ Cayan, D. R., T. Das, D. W. Pierce, T. P. Barnett, M. Tyree, and A. Gershunov, 2010: Future
²⁵² dryness in the southwest us and the hydrology of the early 21st century drought. *Proceedings of*
²⁵³ *the National Academy of Sciences*, **107** (50), 21 271–21 276.

²⁵⁴ Cayan, D. R., K. T. Redmond, and L. G. Riddle, 1999: ENSO and hydrologic extremes in the
²⁵⁵ western United States*. *Journal of Climate*, **12** (9), 2881–2893.

²⁵⁶ Cayan, D. R., and R. H. Webb, 1993: El niño/southern oscillation and streamflow in the western
²⁵⁷ united states.

- 258 Dennis, J., and Coauthors, 2011: CAM-SE: A scalable spectral element dynamical core for the
259 Community Atmosphere Model. *International Journal of High Performance Computing Applications*, 1094342011428142.
- 260
- 261 Deser, C., A. Phillips, V. Bourdette, and H. Teng, 2012: Uncertainty in climate change projections:
262 the role of internal variability. *Climate Dynamics*, **38** (3-4), 527–546.
- 263 Dettinger, M., 2011: Climate change, atmospheric rivers, and floods in California—a multimodel
264 analysis of storm frequency and magnitude changes1. Wiley Online Library.
- 265 Diffenbaugh, N. S., J. S. Pal, R. J. Trapp, and F. Giorgi, 2005: Fine-scale processes regulate the
266 response of extreme events to global climate change. *Proceedings of the National Academy of
267 Sciences of the United States of America*, **102** (44), 15 774–15 778.
- 268 Duli re, V., Y. Zhang, and E. P. Salath  Jr, 2011: Extreme Precipitation and Temperature over the
269 US Pacific Northwest: A Comparison between Observations, Reanalysis Data, and Regional
270 Models*. *Journal of Climate*, **24** (7), 1950–1964.
- 271 Easterling, D. R., G. A. Meehl, C. Parmesan, S. A. Changnon, T. R. Karl, and L. O. Mearns, 2000:
272 Climate extremes: observations, modeling, and impacts. *science*, **289** (5487), 2068–2074.
- 273 Fedorov, A. V., and S. G. Philander, 2000: Is el ni o changing? *Science*, **288** (5473), 1997–2002.
- 274 Fox-Rabinovitz, M., J. C t , B. Dugas, M. D qu , and J. L. McGregor, 2006: Variable resolution
275 general circulation models: Stretched-grid model intercomparison project (SGMIP). *Journal of
276 Geophysical Research: Atmospheres (1984–2012)*, **111** (D16).
- 277 Fox-Rabinovitz, M. S., G. L. Stenchikov, M. J. Suarez, and L. L. Takacs, 1997: A finite-
278 difference GCM dynamical core with a variable-resolution stretched grid. *Monthly weather
279 review*, **125** (11), 2943–2968.

- 280 Frei, C., R. Schöll, S. Fukutome, J. Schmidli, and P. L. Vidale, 2006: Future change of precipitation extremes in Europe: Intercomparison of scenarios from regional climate models. *Journal*
281
282 *of Geophysical Research: Atmospheres (1984–2012)*, **111** (D6).
- 283 Gates, W. L., 1992: AMIP: The Atmospheric Model Intercomparison Project. *Bulletin of the*
284 *American Meteorological Society*, **73**, 1962–1970.
- 285 Gershunov, A., and T. P. Barnett, 1998: Interdecadal modulation of enso teleconnections. *Bulletin*
286 *of the American Meteorological Society*, **79** (12), 2715–2725.
- 287 Guilyardi, E., A. Wittenberg, A. Fedorov, M. Collins, C. Wang, A. Capotondi, G. J. Van Olden-
288 borgh, and T. Stockdale, 2009: Understanding el niño in ocean-atmosphere general circulation
289 models. *Bulletin of the American Meteorological Society*, **90** (3), 325.
- 290 Hamlet, A. F., and D. P. Lettenmaier, 2007: Effects of 20th century warming and climate variability
291 on flood risk in the western us. *Water Resources Research*, **43** (6).
- 292 Hegerl, G. C., F. W. Zwiers, P. A. Stott, and V. V. Kharin, 2004: Detectability of anthropogenic
293 changes in annual temperature and precipitation extremes. *Journal of Climate*, **17** (19), 3683–
294 3700.
- 295 Huang, X., A. M. Rhoades, P. A. Ullrich, and C. M. Zarzycki, 2016: An evaluation of the vari-
296 able resolution-cesm for modeling california’s climate. *Journal of Advances in Modeling Earth*
297 *Systems*.
- 298 Hurrell, J. W., J. J. Hack, D. Shea, J. M. Caron, and J. Rosinski, 2008: A new sea surface temper-
299 ature and sea ice boundary dataset for the Community Atmosphere Model. *Journal of Climate*,
300 **21** (19), 5145–5153.

- 301 Hurrell, J. W., and Coauthors, 2013: The community earth system model: A framework for col-
302 laborative research. *Bulletin of the American Meteorological Society*, **94** (9), 1339–1360.
- 303 Joshi, M. M., J. M. Gregory, M. J. Webb, D. M. Sexton, and T. C. Johns, 2008: Mechanisms for
304 the land/sea warming contrast exhibited by simulations of climate change. *Climate Dynamics*,
305 **30** (5), 455–465.
- 306 Kahya, E., and J. A. Dracup, 1994: The influences of type 1 el nino and la nina events on stream-
307 flows in the pacific southwest of the united states. *Journal of Climate*, **7** (6), 965–976.
- 308 Kao, H.-Y., and J.-Y. Yu, 2009: Contrasting eastern-pacific and central-pacific types of enso.
309 *Journal of Climate*, **22** (3), 615–632.
- 310 Kharin, V. V., F. W. Zwiers, X. Zhang, and G. C. Hegerl, 2007: Changes in temperature and
311 precipitation extremes in the IPCC ensemble of global coupled model simulations. *Journal of*
312 *Climate*, **20** (8), 1419–1444.
- 313 Kim, J., 2005: A projection of the effects of the climate change induced by increased co2 on
314 extreme hydrologic events in the western us. *Climatic Change*, **68** (1-2), 153–168.
- 315 Laprise, R., and Coauthors, 2008: Challenging some tenets of regional climate modelling. *Meteo-*
316 *rology and Atmospheric Physics*, **100** (1-4), 3–22.
- 317 Leung, L. R., L. O. Mearns, F. Giorgi, and R. L. Wilby, 2003a: Regional climate research: needs
318 and opportunities. *Bulletin of the American Meteorological Society*, **84** (1), 89–95.
- 319 Leung, L. R., and Y. Qian, 2009: Atmospheric rivers induced heavy precipitation and flooding in
320 the western US simulated by the WRF regional climate model. *Geophysical research letters*,
321 **36** (3).

- 322 Leung, L. R., Y. Qian, and X. Bian, 2003b: Hydroclimate of the western United States based on
323 observations and regional climate simulation of 1981-2000. Part I: Seasonal statistics. *Journal*
324 *of Climate*, **16 (12)**, 1892–1911.
- 325 McDonald, A., 2003: Transparent boundary conditions for the shallow-water equations: testing in
326 a nested environment. *Monthly weather review*, **131 (4)**, 698–705.
- 327 Mesinger, F., and K. Veljovic, 2013: Limited area NWP and regional climate modeling: a test
328 of the relaxation vs Eta lateral boundary conditions. *Meteorology and Atmospheric Physics*,
329 **119 (1-2)**, 1–16.
- 330 Min, S.-K., X. Zhang, F. W. Zwiers, and G. C. Hegerl, 2011: Human contribution to more-intense
331 precipitation extremes. *Nature*, **470 (7334)**, 378–381.
- 332 Neale, R. B., and Coauthors, 2010a: Description of the NCAR community atmosphere model
333 (CAM 5.0). *NCAR Tech. Note NCAR/TN-486+ STR*.
- 334 Neale, R. B., and Coauthors, 2010b: Description of the NCAR Community Atmosphere Model
335 (CAM 5.0). NCAR Technical Note NCAR/TN-486+STR, National Center for Atmospheric Re-
336 search, Boulder, Colorado, 268 pp.
- 337 Neiman, P. J., F. M. Ralph, G. A. Wick, J. D. Lundquist, and M. D. Dettinger, 2008: Meteorolog-
338 ical characteristics and overland precipitation impacts of atmospheric rivers affecting the west
339 coast of north america based on eight years of ssm/i satellite observations. *Journal of Hydrom-
340 eteorology*, **9 (1)**, 22–47.
- 341 O’Gorman, P. A., and T. Schneider, 2009: The physical basis for increases in precipitation ex-
342 tremes in simulations of 21st-century climate change. *Proceedings of the National Academy of
343 Sciences*, **106 (35)**, 14 773–14 777.

- 344 Oleson, K., and Coauthors, 2010: Technical description of version 4.0 of the Community Land
345 Model (CLM). NCAR Technical Note NCAR/TN-478+STR, National Center for Atmospheric
346 Research, Boulder, Colorado, 257 pp. doi:10.5065/D6FB50WZ.
- 347 Pierce, D. W., 2002: The role of sea surface temperatures in interactions between enso and the
348 north pacific oscillation. *Journal of climate*, **15** (11), 1295–1308.
- 349 Ralph, F. M., P. J. Neiman, and G. A. Wick, 2004: Satellite and caljet aircraft observations of
350 atmospheric rivers over the eastern north pacific ocean during the winter of 1997/98. *Monthly
351 Weather Review*, **132** (7), 1721–1745.
- 352 Rauscher, S. A., E. Coppola, C. Piani, and F. Giorgi, 2010: Resolution effects on regional climate
353 model simulations of seasonal precipitation over Europe. *Climate dynamics*, **35** (4), 685–711.
- 354 Rauscher, S. A., T. D. Ringler, W. C. Skamarock, and A. A. Mirin, 2013: Exploring a Global
355 Multiresolution Modeling Approach Using Aquaplanet Simulations. *Journal of Climate*, **26** (8),
356 2432–2452.
- 357 Rhoades, A. M., X. Huang, P. A. Ullrich, and C. M. Zarzycki, 2015: Characterizing Sierra Nevada
358 snowpack using variable-resolution CESM. *Journal of Applied Meteorology and Climatology*,
359 (2015).
- 360 Riahi, K., and Coauthors, 2011: RCP 8.5A scenario of comparatively high greenhouse gas emis-
361 sions. *Climatic Change*, **109** (1-2), 33–57.
- 362 Rowell, D. P., and R. G. Jones, 2006: Causes and uncertainty of future summer drying over europe.
363 *Climate Dynamics*, **27** (2-3), 281–299.

- 364 Salathé Jr, E. P., R. Steed, C. F. Mass, and P. H. Zahn, 2008: A High-Resolution Climate Model
365 for the US Pacific Northwest: Mesoscale Feedbacks and Local Responses to Climate Change*.
366 *Journal of Climate*, **21** (21), 5708–5726.
- 367 Scoccimarro, E., M. Zampieri, A. Bellucci, A. Navarra, and Coauthors, 2013: Heavy precipitation
368 events in a warmer climate: results from CMIP5 models. *Journal of climate*.
- 369 Seneviratne, S. I., and Coauthors, 2012: Changes in climate extremes and their impacts on the
370 natural physical environment. *Managing the risks of extreme events and disasters to advance*
371 *climate change adaptation*, 109–230.
- 372 Sillmann, J., V. Kharin, F. Zwiers, X. Zhang, and D. Bronaugh, 2013: Climate extremes indices
373 in the cmip5 multimodel ensemble: Part 2. future climate projections. *Journal of Geophysical*
374 *Research: Atmospheres*, **118** (6), 2473–2493.
- 375 Simmons, A., K. Willett, P. Jones, P. Thorne, and D. Dee, 2010: Low-frequency variations
376 in surface atmospheric humidity, temperature, and precipitation: Inferences from reanalyses
377 and monthly gridded observational data sets. *Journal of Geophysical Research: Atmospheres*,
378 **115** (D1).
- 379 Singh, D., M. Tsiang, B. Rajaratnam, and N. S. Diffenbaugh, 2013: Precipitation extremes over the
380 continental United States in a transient, high-resolution, ensemble climate model experiment.
381 *Journal of Geophysical Research: Atmospheres*, **118** (13), 7063–7086.
- 382 Staniforth, A. N., and H. L. Mitchell, 1978: A variable-resolution finite-element technique for
383 regional forecasting with the primitive equations. *Monthly Weather Review*, **106** (4), 439–447.

- 384 Taylor, M. A., 2011: Conservation of mass and energy for the moist atmospheric primitive equa-
385 tions on unstructured grids. *Numerical Techniques for Global Atmospheric Models*, Springer,
386 357–380.
- 387 Tebaldi, C., K. Hayhoe, J. M. Arblaster, and G. A. Meehl, 2006: Going to the extremes. *Climatic
388 change*, **79 (3-4)**, 185–211.
- 389 Trenberth, K. E., 2011: Changes in precipitation with climate change. *Climate Research*, **47 (1)**,
390 123.
- 391 Trenberth, K. E., A. Dai, R. M. Rasmussen, and D. B. Parsons, 2003: The changing character of
392 precipitation. *Bulletin of the American Meteorological Society*, **84 (9)**, 1205–1217.
- 393 Wehner, M. F., 2013: Very extreme seasonal precipitation in the NARCCAP ensemble: model
394 performance and projections. *Climate Dynamics*, **40 (1-2)**, 59–80.
- 395 Wehner, M. F., R. L. Smith, G. Bala, and P. Duffy, 2010: The effect of horizontal resolution
396 on simulation of very extreme US precipitation events in a global atmosphere model. *Climate
397 dynamics*, **34 (2-3)**, 241–247.
- 398 Yoon, J.-H., S. S. Wang, R. R. Gillies, B. Kravitz, L. Hipps, and P. J. Rasch, 2015: Increasing
399 water cycle extremes in California and in relation to El Niño cycle under global warming. *Nature
400 communications*, **6**.
- 401 Zarzycki, C. M., C. Jablonowski, and M. A. Taylor, 2014: Using Variable-Resolution Meshes
402 to Model Tropical Cyclones in the Community Atmosphere Model. *Monthly Weather Review*,
403 **142 (3)**, 1221–1239.

- ⁴⁰⁴ Zarzycki, C. M., C. Jablonowski, D. R. Thatcher, and M. A. Taylor, 2015: Effects of localized grid
⁴⁰⁵ refinement on the general circulation and climatology in the Community Atmosphere Model.
⁴⁰⁶ *Journal of Climate*, (2015).
- ⁴⁰⁷ Zhang, X., L. Alexander, G. C. Hegerl, P. Jones, A. K. Tank, T. C. Peterson, B. Trewin, and
⁴⁰⁸ F. W. Zwiers, 2011: Indices for monitoring changes in extremes based on daily temperature and
⁴⁰⁹ precipitation data. *Wiley Interdisciplinary Reviews: Climate Change*, **2** (6), 851–870.
- ⁴¹⁰ Zhang, X., J. Wang, F. W. Zwiers, and P. Y. Groisman, 2010: The influence of large-scale climate
⁴¹¹ variability on winter maximum daily precipitation over North America. *Journal of Climate*,
⁴¹² **23** (11), 2902–2915.
- ⁴¹³ (update topo here)
- ⁴¹⁴ (add fraction in this figure)
- ⁴¹⁵ (update the figure, separate the IVT and IWV for non-extreme precipitation days and extreme
⁴¹⁶ precipitation ones)

417 LIST OF TABLES

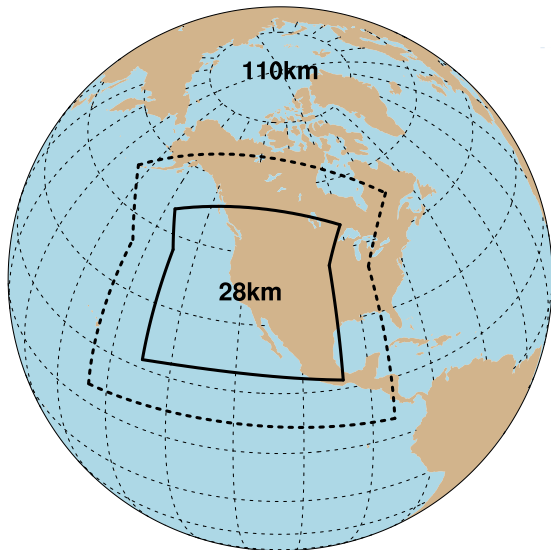
TABLE 1. Precipitation indices used in this study.

Name	Definition
Pr	Mean daily precipitation averaged over each time period. unit: mm/day
SDII	Simple precipitation intensity index: Precipitation amount/rainy days ($Pr > 1$ mm). unit: mm/day
R1mm	Number of days with $Pr > 1$ mm per year averaged over each time period
R5mm	Number of days with $Pr > 1$ mm and $Pr \leq < 5$ mm per year averaged over each time period
R10mm	Number of days with $Pr > 5$ mm and $Pr \leq < 10$ mm per year averaged over each time period
R20mm	Number of days with $Pr > 10$ mm and $Pr \leq < 20$ mm per year averaged over each time period
R40mm	Number of days with $Pr > 20$ mm and $Pr \leq < 40$ mm per year averaged over each time period
Rxmm	Number of days with $Pr > 40$ mm per year averaged over each time period

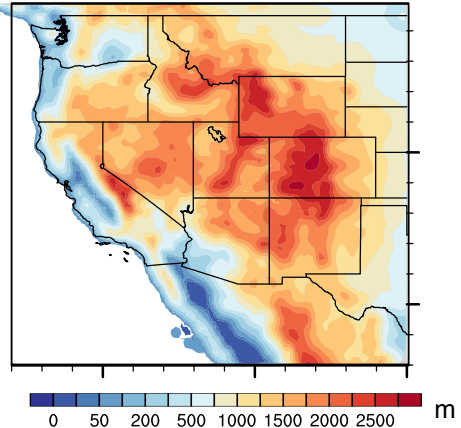
419 **LIST OF FIGURES**

420 Fig. 1.	(a) The approximate grid spacing used for the VR-CESM 0.25° mesh. (b) A depiction of 421 the transition from the global 1° resolution mesh through two layers of refinement to 0.25° . 422 (c) Topography height over study area.	25
423 Fig. 2.	The mean precipitation and other related indices from VR-CESM and reference datasets 424 over 1980-2005.	26
425 Fig. 3.	The mean precipitation (Pr), 2m average temperature ($T2avg$), and 2m relative humidity 426 (RH) averaged over each time period.	27
427 Fig. 4.	Differences of precipitation behaviors from past to future over western U.S. averaged over 428 each time period.	28
429 Fig. 5.	Difference of precipitation behaviors between warm and cool phases of ENSO from past to 430 future over western U.S. averaged over each time period.	29
431 Fig. 6.	Changes of moisture flux at 850hPa, IVT and IWV for simulations under different time 432 period and different phases of ENSO.	30

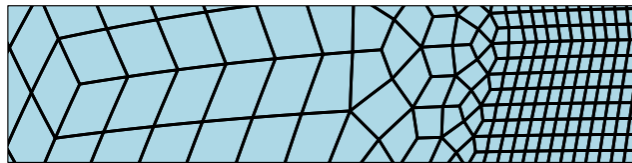
(a) VR-CESM 0.25°



(c) Topography height



(b)



433 FIG. 1. (a) The approximate grid spacing used for the VR-CESM 0.25° mesh.
434 (b) A depiction of the transition from the global 1° resolution mesh through two layers of refinement to 0.25° .
435 (c) Topography height over study area.

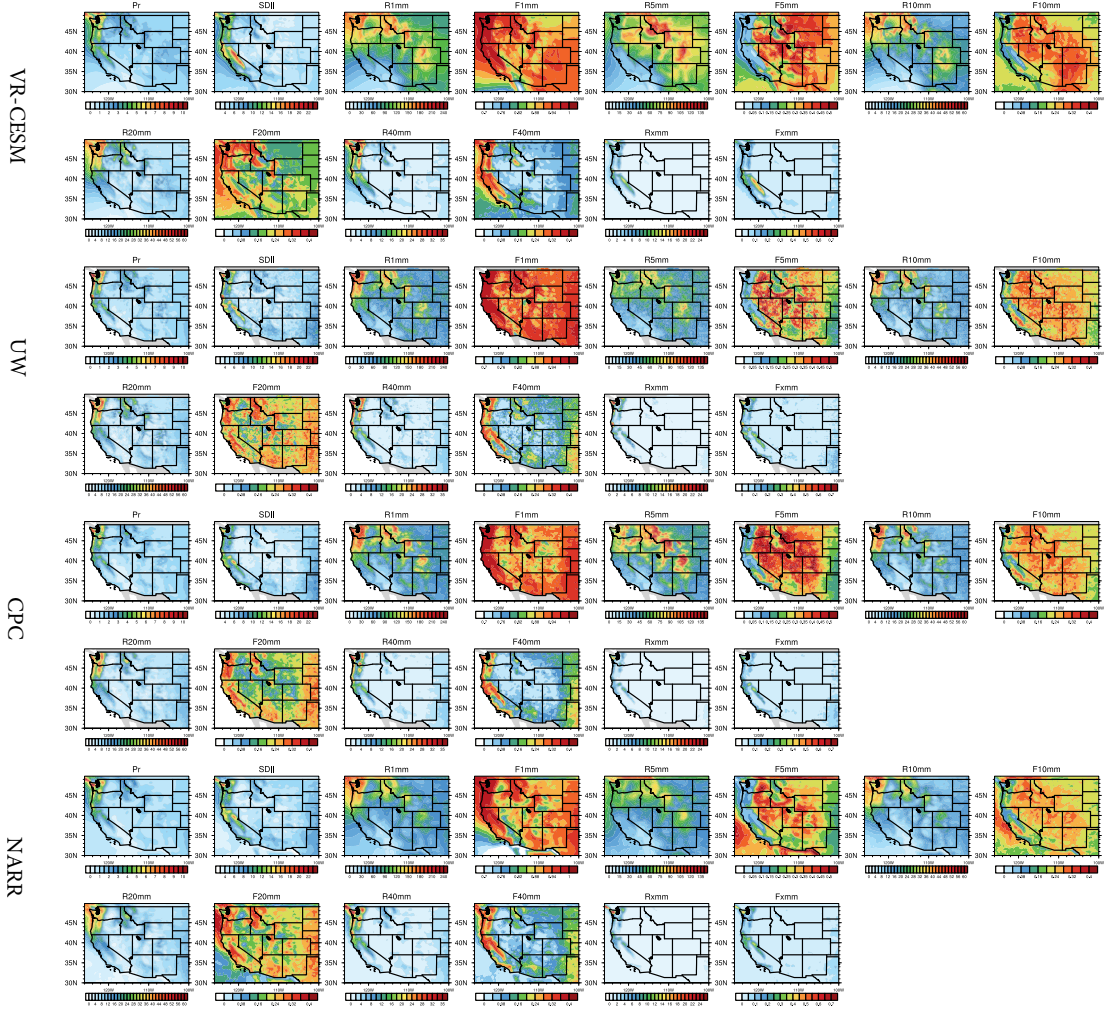
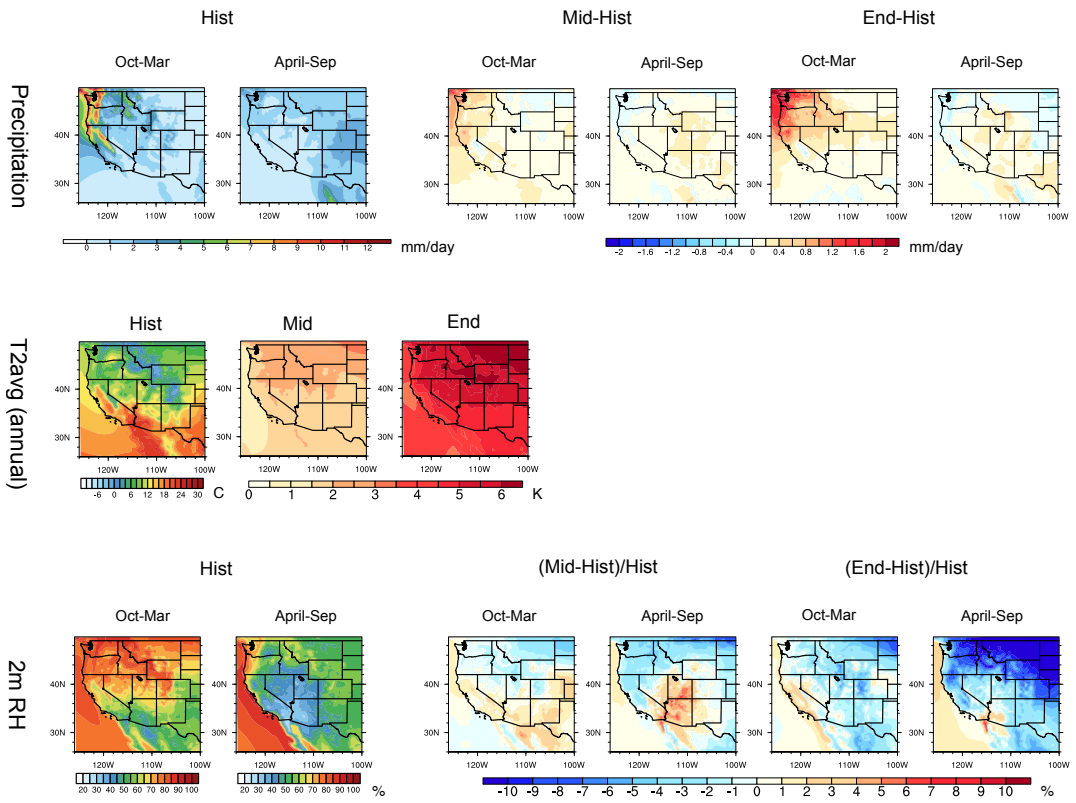
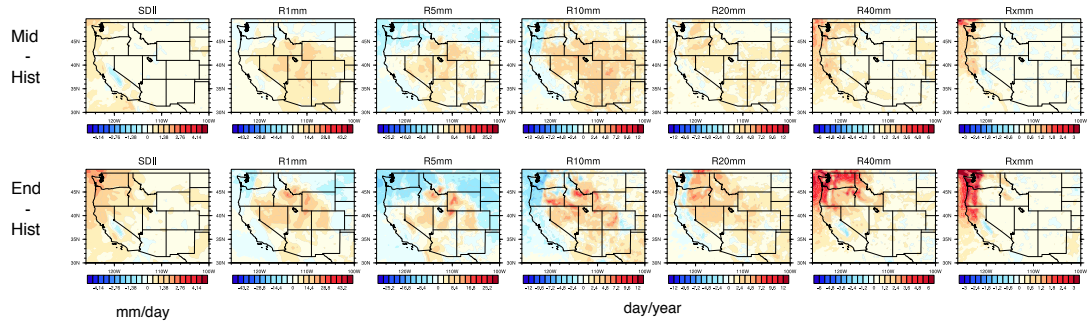


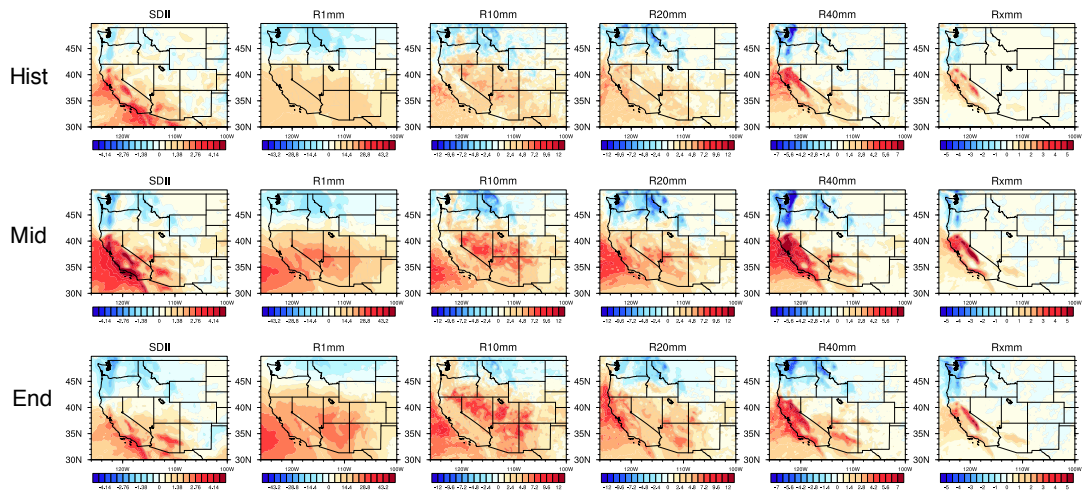
FIG. 2. The mean precipitation and other related indices from VR-CESM and reference datasets over 1980-2005.



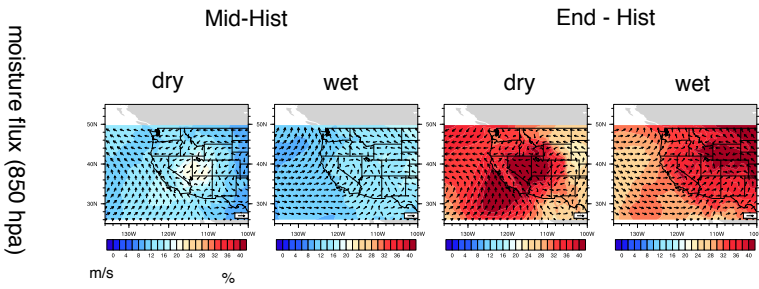
436 FIG. 3. The mean precipitation (Pr), 2m average temperature (T_{2avg}), and 2m relative humidity (RH) aver-
 437 aged over each time period.



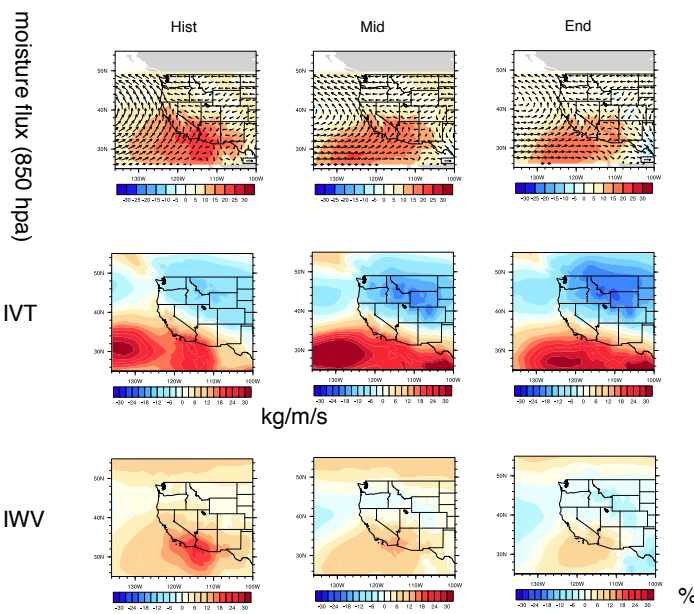
438 FIG. 4. Differences of precipitation behaviors from past to future over western U.S. averaged over each time
 439 period.



440 FIG. 5. Difference of precipitation behaviors between warm and cool phases of ENSO from past to future
 441 over western U.S. averaged over each time period.



El Nino - La Nina



442 FIG. 6. Changes of moisture flux at 850hPa, IVT and IWV for simulations under different time period and
443 different phases of ENSO.